Available online at www.sciencedirect.com
SCIENCE DIRECT®
Journal of Solid State Chemistry 178 (2005) 3500–3506
JOURNAL OF SOLID STATE CHEMISTRY
www.elsevier.com/locate/jssc

Preparation and photocatalytic activity of $ZnO/TiO_2/SnO_2$ mixture

Cun Wang[a], Bo-Qing Xu[a,*], Xinming Wang[b], Jincai Zhao[c]

[a]*Innovative Catalysis Program, Key Lab of Organic Optoelectronics & Molecular Engineering, Department of Chemistry, Tsinghua University, Beijing 100084, China*
[b]*Guangzhou Institute of Geochemistry, Chinese Academy of Sciences, Guangzhou 510640, China*
[c]*Institute of Chemistry, Chinese Academy of Sciences, Beijing 100080, China*

Received 12 June 2005; received in revised form 29 August 2005; accepted 6 September 2005
Available online 5 October 2005

Abstract

$ZnO/TiO_2/SnO_2$ mixture was prepared by mixing its component solid oxides ZnO, TiO_2 and SnO_2 in the molar ratio of 4:1:1, followed by calcining the solid mixture at 200–1300 °C. The products and solid-state reaction process during the calcinations were characterized with powder X-ray diffraction (XRD), thermogravimetric and differential thermal analysis (TG-DTA), UV-Vis diffuse reflectance spectroscopy (UV-Vis DRS) and Brunauer–Emmett–Teller measurement of specific surface area. Neither solid-state reaction nor change of crystal phase composition took place among the ZnO, TiO_2 and SnO_2 powders on the calcinations up to 600 °C. However, formation of the inverse spinel Zn_2TiO_4 and Zn_2SnO_4 was detected at 700–900 and 1100–1200 °C, respectively. Further increase of the calcination temperature enabled the mixture to form a single-phase solid solution $Zn_2Ti_{0.5}Sn_{0.5}O_4$ with an inverse spinel structure in the space group of $O_h^7 - Fd3m$. The $ZnO/TiO_2/SnO_2$ mixture was photocatalytically active for the degradation of methyl orange in water; its photocatalytic mass activity was 16.4 times that of SnO_2, 2.0 times that of TiO_2, and 0.92 times that of ZnO after calcination at 500 °C for 2 h. But, the mass activity of the mixture decreased with increasing the calcination temperature at above 700 °C because of the formation of the photoinactive Zn_2TiO_4, Zn_2SnO_4 and $Zn_2Ti_{0.5}Sn_{0.5}O_4$. The sample became completely inert for the photocatalysis after prolonged calcination at 1300 °C (42 h), since all of the active component oxides were reacted to form the solid solution $Zn_2Ti_{0.5}Sn_{0.5}O_4$ with no photocatalytic activity.
© 2005 Elsevier Inc. All rights reserved.

Keywords: Zinc oxide; Titanium dioxide; Tin dioxide; Mixed oxides; Solid-state reaction; Photocatalysis; Inverse spinel; $Zn_2Ti_{0.5}Sn_{0.5}O_4$

1. Introduction

Photocatalytic degradation of organic pollutants in water and air using semiconductors, such as TiO_2 and ZnO, has attracted extensive attention in the past two decades [1]. Previous studies have proved that such semiconductors can degrade most kinds of persistent organic pollutants, such as detergents, dyes, pesticides and volatile organic compounds, under ultraviolet (UV) light irradiation. A photocatalytic process is based on the generation of electron–hole pairs by means of band-gap radiation that can give rise to redox reactions with the species adsorbed on the surface of the photocatalysts. In principle the coupling of different semiconductor oxides seems useful in order to achieve a more efficient electron–hole pair separation under irradiation and, consequently, a higher photocatalytic activity. A large variety of coupled polycrystalline or colloidal semiconductor systems, in which the particles adhere to each other in so-called "sandwich structure" or present in "core-shell geometry", have been prepared and used for many photocatalytic reactions [2–9]. Typical examples of such couplings are SnO_2/TiO_2 [2,3], ZnO/TiO_2 [4] and ZnO/SnO_2 [5,6].

For SnO_2/TiO_2, a stearic acid method was used by Yang et al. to prepare a nanostructured SnO_2/TiO_2 binary oxide [2]. It was found that the binary oxide showed higher photocatalytic activity than Degussa P-25 TiO_2 in the photocatalytic degradation of methyl orange (MO). Shi et al. reported that ultrafine SnO_2/TiO_2 coupled particles prepared by a homogenous precipitation method also

*Corresponding author. Fax: +86 10 62792122.
E-mail addresses: wangcun@mail.tsinghua.edu.cn (C. Wang), bqxu@mail.tsinghua.edu.cn (B.-Q. Xu).

0022-4596/$ - see front matter © 2005 Elsevier Inc. All rights reserved.
doi:10.1016/j.jssc.2005.09.005

exhibited higher activity than that of the corresponding ultrafine pure TiO_2 for the photocatalytic degradation of azo dye active red X-3B [3].

In the case of ZnO/TiO_2, Marci et al. [4] discovered that the polycrystalline SnO_2/TiO_2 powders prepared by loading the anatase or rutile TiO_2 with ZnO from $Zn(NO_3)_2 \cdot 6H_2O$ or $Zn(CH_3COO)_2 \cdot 2H_2O$ precursors were not so beneficial, as would be expected on the basis of their intrinsic electronic properties, for the photocatalytic degradation of 4-nitrophenol in aqueous medium, although some of the powder samples showed activities slightly higher than those of the corresponding single TiO_2 and ZnO.

For ZnO/SnO_2, the composite ZnO/SnO_2 nanocrystalline particles prepared with colloidal SnO_2 and ZnO precursors by Bandara et al. [5] exhibited improved photocatalytic activity for the sensitized degradation of dyes (e.g., Eosin Y), compared to those of the single oxides (ZnO, SnO_2 or TiO_2). In an earlier work of Wang et al. coupled nanosized ZnO/SnO_2 samples prepared by co-precipitation method also showed higher activity than ZnO and SnO_2 in the photocatalytic degradation of MO in aqueous solution [6].

An increase of the lifetime of photogenerated electron–hole pairs in the coupled oxides, due to the hole and electron transfer between the two coupling semiconductors, is crucial to the catalytic activity enhancement in many photocatalytic reaction systems. Nevertheless, it should be considered that the photocatalyitc activity also strongly depends on the bulk and surface physicochemical properties of the semiconductor catalysts, such as the phase composition, defects (both in the bulk and at the surfaces) and surface area. Consequently, useful information on the photocatalysts can also be obtained by the characterizations that are frequently used in conventional thermal catalysts.

In this work, polycrystalline $ZnO/TiO_2/SnO_2$ mixture powders were prepared by mixing stoichiometric amounts of the ZnO, TiO_2 and SnO_2 powders followed by heat-treatment at elevated temperatures. The mixture powders were then characterized by X-ray diffraction (XRD), thermogravimetric and differential thermal analysis (TG-DTA), specific surface area determination with the Brunauer–Emmett–Teller (BET) method and UV-visible diffuse reflectance spectroscopy (UV-Vis DRS). The results were used to explain the activity change of the calcined $ZnO/TiO_2/SnO_2$ mixtures for the photocatalytic degradation of MO in aqueous solution.

2. Experimental

2.1. Preparation of the $ZnO/TiO_2/SnO_2$ mixtures

The $ZnO/TiO_2/SnO_2$ mixtures were prepared from a powder mixture of the constituent oxides, at the molar ratio of $ZnO:TiO_2:SnO_2 = 4:1:1$, by the solid-state reaction at elevated temperatures. The starting materials, ZnO (zincite, >99.9 wt%, particle size ca. 0.5 μm and BET surface area of 3.3 m^2/g), TiO_2 (anatase, >99.8 wt%, particle size ca. 200 nm and BET surface area of 11.4 m^2/g) and SnO_2 (cassiterite, >99.9 wt%, particle size ca. 250 nm and BET surface area of 10.5 m^2/g), were analytic grade reagents purchased from Beijing Chemical Factory (China) and were used as supplied. The mixture was ground thoroughly in an agate mortar for about 2 h, and then divided into several parts in corundum crucibles, followed by calcination for different durations at elevated temperatures in the range of 200–1300 °C. The calcined samples were hand-ground again to prepare the powdered mixture for photocatalysis measurements.

2.2. Characterizations of the $ZnO/TiO_2/SnO_2$ mixtures

XRD patterns of the $ZnO/TiO_2/SnO_2$ mixtures were recorded in ambient air at room temperature with a Bruker D8 Advance diffractometer with Cu $K\alpha$ radiation ($\lambda = 1.5406$ Å); the accelerating voltage, emission current, and scanning speed were 40 kV, 40 mA and 6 °/min, respectively. The TG-DTA analysis was conducted with a sample loading of 44.33 mg on a Setaram TGA/DTA92 instrument in static ambient air heated at a heating rate of 10 °C/min from 50 to 1400 °C. The specific surface areas (S_{BET}) were determined by using nitrogen adsorption data at 77 K obtained by a Micromeritics ASAP 2010 system with multipoint BET method. In order to increase the accuracy of the measured surface area data, we intentionally used a higher sample loading (up to 5 g for the sample with the lowest specific surface area) to ensure that the measured sample surface area was larger than 1.0 m^2, which is within the accuracy of the instrument. The UV-Vis DRS were recorded on a Hitachi U-3010 spectrophotometer, using pure $BaSO_4$ powders as the reference sample.

2.3. Evaluation of photocatalytic activity

The photodegradation of MO in water was used to evaluate the catalytic activity of the $ZnO/TiO_2/SnO_2$ mixture powders. The photocatalytic reactor consists of two parts: a 100 mL columned glass bottle and a 500 W high pressure Hg lamp (UV light) with a light intensity of 2.9×10^4 μW/cm^2 at the middle of the axis of the bottle and a maximum emission wavelength of about 365 nm. The lamp was positioned in parallel to the glass bottle. In all experiments, the reaction temperature was kept at 25 ± 2 °C.

Reaction suspensions were prepared by adding the photocatalyst powders into the aqueous MO solutions of 100 mL. Prior to the photoirradiation, the suspensions were ultrasonically sonicated for 30 min and then magnetically stirred under dark for 10 min to establish an adsorption/desorption equilibrium. The suspensions containing MO and photocatalysts were then irradiated by the UV light.

During the photodegradation, the concentration of MO in the solution was monitored by sampling a small amount (ca. 2 mL) of the reaction suspension at different times. After separation of the solid catalysts from the suspensions by centrifuging at 9000 rpm for 10 min followed by filtration through a 0.2 μm millipore filter, the MO concentrations in the filtrates were analyzed by UV-Vis spectroscopy with a Unico UV-2102 PC UV-Vis spectrophotometer at its maximum absorption wavelength (ca. 464 nm).

3. Results and discussion

The XRD patterns of the $ZnO/TiO_2/SnO_2$ mixture powders after different calcinations are shown in Fig. 1. The data show that both the phase composition and the growth of crystals in the $ZnO/TiO_2/SnO_2$ mixture are sensitive to the calcination condition. After the calcinations for 2 h at 300 °C (not shown), 500 and 600 °C (not shown), the mixture showed no other phases except those of the starting materials: ZnO (zincite), TiO_2 (anatase) and SnO_2 (cassiterite). A reaction between ZnO and TiO_2 to form Zn_2TiO_4 (cubic) (JCPDS 77-0014) took place during the calcinations at 700–900 °C, which agrees with the observations in a number of earlier reports [10–12]. However, the formation of $ZnTiO_3$ (hexagonal) and/or $Zn_2Ti_3O_8$ (cubic), which were reported in those earlier works [10–12], was not detected in the XRD patterns of Fig. 1. The characteristic diffractions of anatase TiO_2 were hardly detectable after the calcination at 800 °C for 2 h (not shown), and they disappeared completely after the calcination at 900 °C for 2 h. To understand the disappearance of the anatase TiO_2, independent calcinations were made on the anatase TiO_2 and the XRD data of this pure TiO_2 (not shown) indicated,

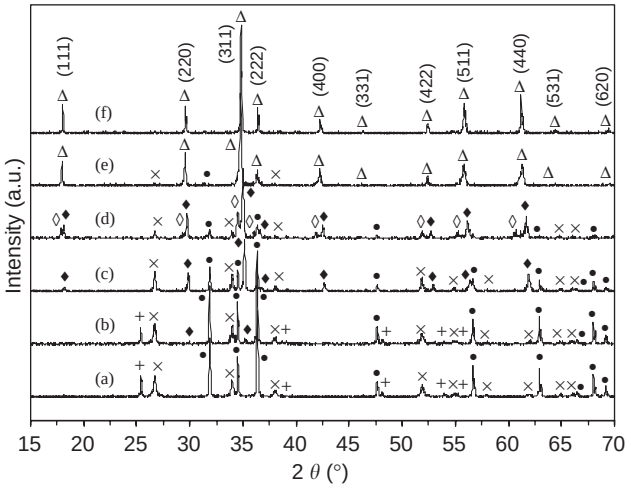

Fig. 1. XRD patterns of the calcined $ZnO/TiO_2/SnO_2$ powder mixtures. The calcination temperature and duration are 500 °C and 2 h (a), 700 °C and 2 h (b), 900 °C and 2 h (c), 1100 °C and 2 h (d), 1300 °C and 2 h (e), and 1300 °C and 42 h (f), respectively. Information on the crystal phase: (+) anatase TiO_2; (×) cassiterite SnO_2; (●) zincite ZnO; (◆) Zn_2TiO_4; (◇) Zn_2SnO_4; and (△) $Zn_2Ti_{0.5}Sn_{0.5}O_4$.

in agreement with the data reported in Ref. [13], that an anatase-to-rutile transformation occurred in between 1000 and 1100 °C. This phase transformation temperature (1000–1100 °C) is higher than the disappearance temperature of TiO_2 in the mixture (800–900 °C). Since no formation of the rutile TiO_2 phase was detected in the calcined mixtures, it is certainly that the disappearance of anatase TiO_2 was not due to a phase transformation of TiO_2. Also, there is least possibility that the TiO_2 could exist in a XRD invisible amorphous state after the calcination at the temperature as high as 900 °C. The disappearance of anatase TiO_2 in the calcined mixture can most reasonably be accounted for by a solid-state reaction between the anatase TiO_2 and ZnO to form Zn_2TiO_4. Although a reaction between the anatase TiO_2 and SnO_2 to form a SnO_2-rich solid solution TiO_2–SnO_2 of the rutile structure [13–17] cannot be completely ruled out, this reaction is little possible since the disappearance of anatase TiO_2 in Fig. 1 was apparently accompanied with a continuous reduction of the ZnO signals and the formation of Zn_2TiO_4 in the calcined mixture. The XRD peaks of Zn_2TiO_4 were intensified when the calcination temperature was raised up to 1000 °C, due to a sintering of the Zn_2TiO_4 crystals.

A further calcination of the mixture at 1100 °C for 2 h resulted in the formation of another new phase Zn_2SnO_4 (cubic) (JCPDS 74-2184), which is consistent with the result in Ref. [18]. A still further increase of the calcination temperature (1200 °C) caused both Zn_2TiO_4 and Zn_2SnO_4 phases to react to form a completely new phase with a set of diffractions at $2\theta = 18.00°$, 29.66°, 34.91°, 36.47°, 42.40°, 52.64°, 56.08°, 61.57°, which may be assigned to a solid solution $Zn_2Ti_xSn_{1-x}O_4$ $(0<x<1)$. The solid-state reaction leading to the formation of $Zn_2Ti_xSn_{1-x}O_4$ $(0<x<1)$ from Zn_2TiO_4 and Zn_2SnO_4 can be expressed as

$$Zn_2TiO_4 + Zn_2SnO_4 \rightarrow Zn_2Ti_xSn_{1-x}O_4 \quad (0<x<1).$$

The formation and growth of the $Zn_2Ti_xSn_{1-x}O_4$ $(0<x<1)$ crystallites continued when the calcination temperature was further increased to 1300 °C when the residual ZnO (zincite) and SnO_2 (cassiterite) almost disappeared, implying that the final product can be approximately viewed as $Zn_2Ti_{0.5}Sn_{0.5}O_4$.

The XRD pattern of the solid solution $Zn_2Ti_{0.5}Sn_{0.5}O_4$ was indexed by referencing to the Zn_2SnO_4 and Zn_2TiO_4 inverse spinels (Fig. 1). It seems that the calcination for 2 h at 1300 °C was not long enough to induce a complete transformation of the $ZnO/TiO_2/SnO_2$ mixture into the solid solution $Zn_2Ti_{0.5}Sn_{0.5}O_4$, which should show a diffraction pattern at $2\theta = 18.04°$, 29.59°, 34.84°, 36.44°, 42.29°, 46.32°, 52.42°, 55.86°, 61.24°, 64.40°, 69.42°. Therefore, the calcination period was extended to 6, 10, 14, 18, 22, 26, 30, 34, 38 and 42 h at 1300 °C, respectively, and it was found that a period of 42 h is sufficient for such a purpose (see Fig. 1). The inverse spinel-like face-centered cubic structure (space group $O_h^7 - Fd3m$) has 8 A_2BX_4 units (A = Zn, B = Ti and Sn, X = O) ($Z = 8$) that involve

a total of 56 atoms [19]. In these inverse spinel structures the cations (Zn^{2+}, Ti^{4+} and Sn^{4+}) could be arranged as $Zn_{tetra}[ZnTi_xSn_{1-x}]_{octa}O_4$, i.e., one half of the Zn^{2+} ions are in the tetrahedral sites; the other half of the Zn^{2+} ions are mixed randomly with the Ti^{4+} and Sn^{4+} ions in the octahedral sites [19,20]. The cubic lattice constant of $Zn_2Ti_{0.5}Sn_{0.5}O_4$, calculated with the software (Diffrac^{plus} Win-Metric Version 3.0) on the X-ray diffractometer, is 8.547 ± 0.003 Å, which is larger than that of Zn_2TiO_4 (8.4450 Å, JCPDS 77-0014) but smaller than that of Zn_2SnO_4 (8.6500 Å, JCPDS 74-2184) due to the difference in radius between Ti^{4+} (0.68 Å) and Sn^{4+} (0.71 Å).

Fig. 2 shows the TG-DTA curves of the starting $ZnO/TiO_2/SnO_2$ mixture. The TG curve revealed no significant weight change in the temperature range of 400–1400 °C. A little weight loss of 0.11 wt% from 99.87 wt% at 400 °C to 99.76 wt% at 1400 °C could imply a formation of low concentration oxygen vacancies during the heat treatment, due to the escape of part of the crystal lattice oxygen from the component single oxides (ZnO, TiO_2, SnO_2) and/or the solid solutions Zn_2TiO_4, Zn_2SnO_4 and $Zn_2Ti_xSn_{1-x}O_4(0<x<1)$. While on the DTA curve, endothermic effects were apparent at above 700 °C, not to mention the strong endothermic peak at ca. 1190 °C. Since the accompanying TG curve suggests no significant formation of volatile products, the endothermic DTA features must be associated with the thermal effects of the solid-state reactions inducing to the formation of Zn_2TiO_4, Zn_2SnO_4 and $Zn_2Ti_xSn_{1-x}O_4(0<x<1)$ from the mixed oxides. This explanation is consistent with the XRD data (Fig. 1) that Zn_2TiO_4 and Zn_2SnO_4 were formed at about 700 and 1100 °C, respectively. In fact, the formation of Zn_2TiO_4 from the ZnO and TiO_2, and that of Zn_2SnO_4 from the ZnO and SnO_2 were found endothermic in the literatures [21,22]. As we mentioned in presenting the XRD data, the thermal effects occurred in the temperature range of 700–1300 °C could not include the anatase-to-rutile

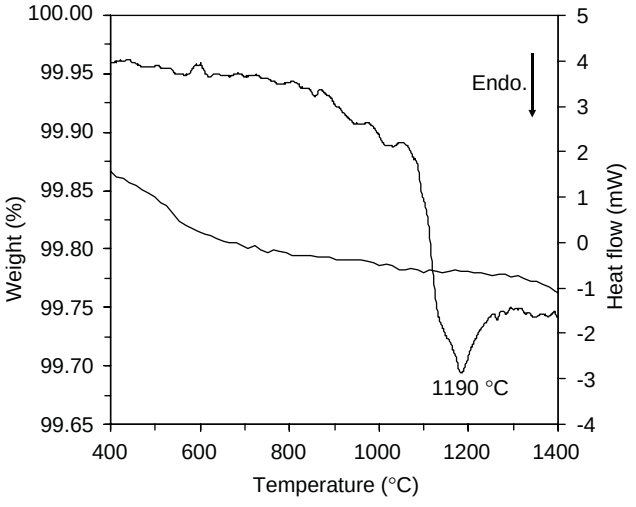

Fig. 2. TG-DTA curves in static ambient air of the $ZnO/TiO_2/SnO_2$ mixture. Starting sample weight: 44.33 mg; heating rate: 10 °C/min.

transformation of TiO_2 because all of the anatase TiO_2 component had reacted with ZnO (at 700–900 °C) to form the Zn_2TiO_4 crystalllites before the anatase-to-rutile transformation could take place (at 1000–1100 °C). Since the Zn_2TiO_4 and Zn_2SnO_4 reacted to form $Zn_2Ti_xSn_{1-x}O_4(0<x<1)$ solid solution at about 1200 °C and the solid solution was found to be the only detectable product after the calcination at 1300 °C, the strong endothermic peak at about 1190 °C should be related with the formation of $Zn_2Ti_xSn_{1-x}O_4(0<x<1)$ from Zn_2TiO_4 and Zn_2SnO_4.

Table 1 gives that the specific surface areas of the calcined $ZnO/TiO_2/SnO_2$ mixture samples. It can be seen that the specific surface area of the $ZnO/TiO_2/SnO_2$ mixture decreased with increasing the calcination temperature due to the changes in the sample particle size (sintering) and in the sample crystal phases. But the effect was little when the calcination temperature is $\leqslant 500$ °C, indicating that no significant sintering occurred among the sample particles below 500 °C. It can be seen that duration of the calcination is also a factor, but not an important one, affecting the specific surface area, since the sample surface area decreased slowly with extending the calcination time.

Fig. 3 shows the UV-Vis diffuse reflectance spectra of the calcined $ZnO/TiO_2/SnO_2$ mixtures. The wavelengths of the absorption edges in the UV-Vis spectra were determined by extrapolating the sharply rising portions and horizontal portions of the UV-Vis curves, defining the absorption edges as the wavelengths at the intersections according to the literatures [6,23]. The samples calcined at 500 °C for 2 h, 700 °C for 2 h, and 1300 °C for 42 h displayed a one-edge absorption, respectively. By contrast, those samples calcined at 900, 1100 and 1300 °C for 2 h displayed a two-edge absorption, respectively. The absorption edges are at 388.8 nm for the sample calcined at 500 °C for 2 h and 389.5 nm for the one calcined at 700 °C for 2 h, corresponding to the apparent band-gap energies of 3.19 and 3.18 eV, respectively. It was reported that both the band-gap energy of ZnO and that of TiO_2 were of 3.20 eV [24], and the absorption edge of SnO_2 occurred in between 1.64 and 3.7 eV [6,25–28]. Therefore, for the sample calcined at 500 °C for 2 h, the absorption curve contains the contributions from each of the oxide components ZnO, TiO_2 and SnO_2, according to the XRD results. The UV-Vis absorption of the sample calcined at 700 °C for 2 h could also be ascribed to the absorptions from ZnO, TiO_2 and SnO_2 because the content of Zn_2TiO_4 in the mixture was not significant. The two absorption edges are at 354.3 and 387.4 nm for the sample calcined at 900 °C for 2 h, 364.3 and 397.9 nm for the one calcined at 1100 °C for 2 h, and 352.0 and 398.6 nm for the one calcined at 1300 °C for 2 h; the corresponding apparent band-gap energies are 3.50 and 3.20 eV, 3.40 and 3.12 eV, and 3.52 and 3.11 eV, respectively. The absorption edges of Zn_2TiO_4 and Zn_2SnO_4 prepared by calcination of ZnO with the stoichiometric amounts of TiO_2 and SnO_2, respectively, are at 355.3 and

Table 1
Specific surface areas (S_{BET}) of the calcined $ZnO/TiO_2/SnO_2$ mixtures with the molar ratio of Zn:Ti:Sn = 4:1:1

Calc. temp. (°C)	As mixed	200	300	500	700	900	1100	1300	1300[a]
S_{BET} (m^2/g)	6.67	6.59	6.43	6.25	5.92	4.32	2.32	0.37	0.23

[a]The duration of the calcination was 42 h for this sample but 2 h for the others.

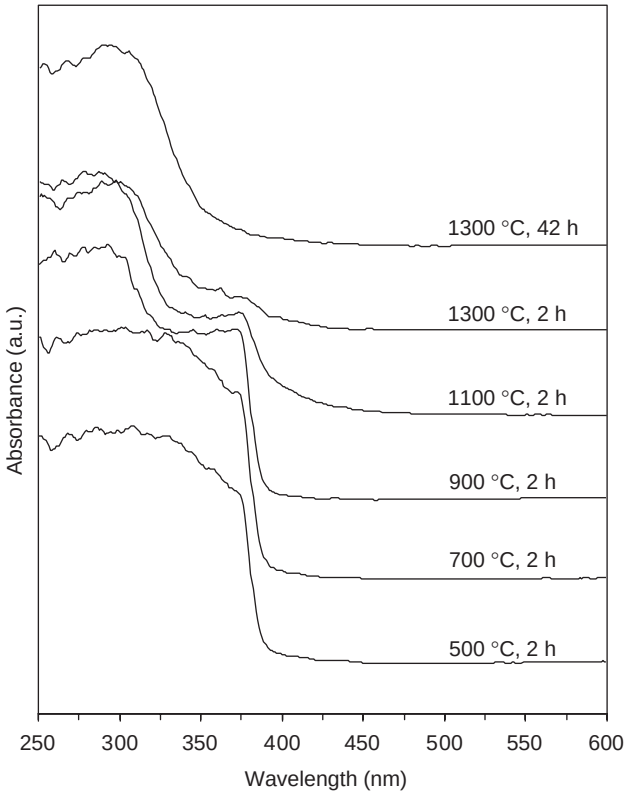

Fig. 3. UV-Vis DRS of the $ZnO/TiO_2/SnO_2$ mixture after the calcinations at the indicated temperatures.

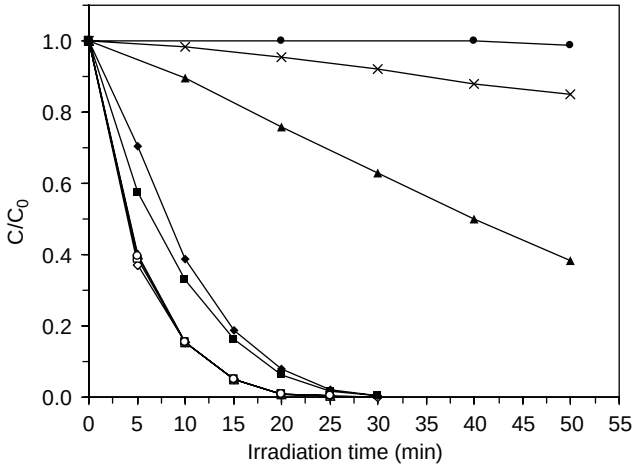

Fig. 4. Dependence of the photocatalytic activity of the $ZnO/TiO_2/SnO_2$ mixture on the calcination temperature and duration. The calcination temperature and duration are raw mixture with no calcinations (◇), 200 °C and 2 h (□), 300 °C and 2 h (○), 500 °C and 2 h (△), 700 °C and 2 h (■), 900 °C and 2 h (◆), 1100 °C and 2 h (▲), 1300 °C and 2 h (×), and 1300 °C and 42 h (●), respectively. Loading of the photocatalysts: 2.5 g/L; concentration of methyl orange: 20 mg/L.

368.0 nm (not shown). These absorptions correspond to the band-gap energies of 3.49 eV for the Zn_2TiO_2 and 3.37 eV for Zn_2SnO_4. Therefore, the absorptions at lower wavelength may be ascribed to the Zn_2TiO_4 for the sample calcined at 900 °C for 2 h, the Zn_2TiO_4 and Zn_2SnO_4 for the sample calcined at 1100 °C for 2 h, and to the $Zn_2Ti_{0.5}Sn_{0.5}O_4$ for the sample calcined at 1300 °C for 2 h. The absorptions at higher wavelength might be attributed to the unreacted ZnO and SnO_2 in these three samples, respectively.

Using the UV-Vis DRS data in Fig. 3 for the solid solution $Zn_2Ti_{0.5}Sn_{0.5}O_4$, which was the only product after the calcination of the starting mixture at 1300 °C for 42 h, the absorption edge of the $Zn_2Ti_{0.5}Sn_{0.5}O_4$ sample is measured at 352.3 nm, corresponding to a band-gap energy of 3.52 eV.

Fig. 4 shows the dependence of the photocatalytic activity of the $ZnO/TiO_2/SnO_2$ mixture on its calcination temperature. The photocatalytic activity decreased slightly with increasing the calcination temperature up to 500 °C, but decreased significantly when the mixture was calcined at higher temperatures, especially at above 900 °C. The mixture became almost inactive after the calcination at 1300 °C.

The photocatalytic activities of the calcined mixtures were normalized with respect to their specific surface area and the obtained areal activities are given in Table 2. The data were expressed by $(C_0-C)/(At)$, where C_0 and C were, respectively, the equilibrium concentrations of MO (mg/L) before and after the light irradiation. And, A was the specific surface area (m^2/g) or loading (g) of the sample for the calculation of the areal or mass activity; t was the reaction time (min) under light irradiation. The reaction time was set as 10 min in the calculation of the areal or mass activities. It is seen that the areal activity remained almost unchanged when the mixture was calcined at temperatures no higher than 900 °C, considering the measurement errors in specific area and photocatalytic activity. The areal activity of the mixture decreased dramatically after it was calcined at 1100 or 1300 °C for 2 h. When the calculation at 1300 °C was prolonged up to 42 h, the calcined mixture became inactive for the photocatalytic reaction.

It is well known that the areal activity of a photocatalyst depends on the density of surface active sites. For the calcinations at temperatures no higher than 500 °C, the

Table 2
Areal photocatalytic activities of the calcined $ZnO/TiO_2/SnO_2$ mixtures with the molar ratio of Zn:Ti:Sn = 4:1:1

Calc. temp. (°C)	As mixed	200	300	500	700	900	1100	1300	1300[a]
Areal activity (mg/(L min m^2))	2.54	2.56	2.63	2.70	2.26	2.84	0.88	0.94	0.043

[a]The duration of the calcination was 42 h for this sample but 2 h for the others.

composition and specific surface area of the $ZnO/TiO_2/SnO_2$ mixture remained unchanged. Therefore, the areal activity of the mixture changed little after the calcinations at those low temperatures. We found that the separately prepared pure Zn_2TiO_4 as well as Zn_2SnO_4 solid solutions were totally inactive for photocatalytic reaction (not shown). As indicated by the XRD results in Fig. 1, the mixture calcined at 700 °C contained some Zn_2TiO_4 from the reaction of TiO_2 and ZnO. Nevertheless, the areal activity of the mixture calcined at 700 °C was just a little lower than those calcined at the lower temperatures (Table 2). This little changed photocatalytic activity suggests that the amount of Zn_2TiO_4 formed in the mixture after the calcination at 700 °C was not very significant. When the mixture was calcined up to about 900 °C, all of the anatase TiO_2 had been converted to the photocatalytically inactive Zn_2TiO_4. Compared with the sample calcined at lower temperatures ($\leqslant$700 °C), the slightly improved areal photocatalytic activity as well as the decreased specific surface area of this sample (calcined at 900 °C) would imply that a considerable amount of the photoactive ZnO still remained unreacted at the sample surface after the calcination at 900 °C, which could be the main contribution for the photocatalysis (the remaining SnO_2 was not enough active as shown in Fig. 5). When the calcination temperature was raised to 1100 °C, the majority of the photoactive ZnO reacted with SnO_2 to form Zn_2SnO_4 and only a very small amount of ZnO was left unreacted, therefore, both the mass (Fig. 4) and areal (Table 2) photocatalytic activities of this calcined mixture became significantly lower than those of the samples calcined at lower temperatures. Although the calcination at 1300 °C for 2 h significantly reduced the mass activity (Fig. 4) of the mixture compared to the calcination at 1100 °C, the areal activity (Table 2) of the mixture did not show significant difference after the calcinations at 1100 and 1300 °C, both for 2 h. Such an insignificant difference in the areal activity is probably arisen from the very small specific surface area (0.37 m^2/g), only a little unreacted photoactive ZnO would enable a meaningful areal activity. However, the mass (Fig. 4) and areal photocatalytic activity data (Table 2) were in agreement to show that the prolonged calcination at 1300 °C (42 h) finally made the mixture inactive for the photocatalysis, which gives an independent evidence that all of the components in the mixture were reacted to form the solid solution $Zn_2Ti_{0.5}Sn_{0.5}O_4$ with no photocatalytic activity. Thus, it could be conclusive that the conduction band energy (E_{CB}) of $Zn_2Ti_{0.5}Sn_{0.5}O_4$ is not positive enough to oxidize the H_2O/OH^- into the OH radicals, which is necessary to initiate a photocatalytic reaction in aqueous solution [1,29].

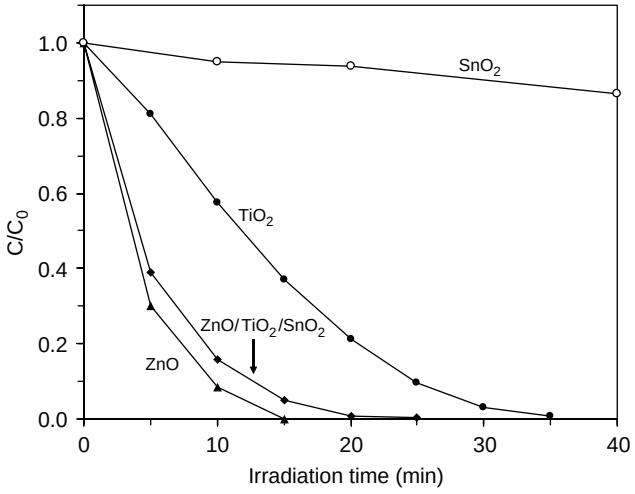

Fig. 5. Comparison of the photocatalytic activities of ZnO, TiO_2, SnO_2 and $ZnO/TiO_2/SnO_2$ after the calcination at 500 °C for 2 h. Loading of the photocatalysts: 2.5 g/L; concentration of methyl orange: 20 mg/L.

A comparison of the photocatalytic activities of the $ZnO/TiO_2/SnO_2$ mixture, and the individual pure ZnO, TiO_2 and SnO_2, all calcined at 500 °C for 2 h, is made in Fig. 5. The specific surface areas were, respectively, 6.25 m^2/g for $ZnO/TiO_2/SnO_2$, 3.20 m^2/g for ZnO, 11.36 m^2/g for TiO_2 and 10.18 m^2/g for SnO_2. Theoretically, the coupled $ZnO/TiO_2/SnO_2$ mixture would exhibit higher photocatalytic activity than any of the corresponding single oxides ZnO, TiO_2 or SnO_2 [29,30], but the data were not totally that case in Fig. 5. The mass photocatalytic activity of the $ZnO/TiO_2/SnO_2$ mixture, obtained according to the method defined previously, is 2.0 times that of TiO_2, 16.4 times that of SnO_2 and 0.92 times that of ZnO, i.e., the $ZnO/TiO_2/SnO_2$ mixture was photocatalytically more active than the pure TiO_2 and SnO_2 but slightly less active than ZnO. This could be caused by the co-presence of the highly active ZnO and little active SnO_2 in the $ZnO/TiO_2/SnO_2$ mixture. Therefore, the present data failed to show the coupling effect in increasing the photocatalytic activity with the $ZnO/TiO_2/SnO_2$ mixture.

4. Conclusions

$ZnO/TiO_2/SnO_2$ mixtures with the molar ratio of $ZnO:TiO_2:SnO_2 = 4:1:1$ were prepared from the component oxide powders ZnO, TiO_2 and SnO_2 by solid-state reaction at elevated temperatures. Formation of the inverse

spinel Zn_2TiO_4 and Zn_2SnO_4 was detected at 700–900 and 1100–1200 °C, respectively. Further calcinations at still higher temperatures enabled the mixture to form a single solid solution $Zn_2Ti_{0.5}Sn_{0.5}O_4$. The $ZnO/TiO_2/SnO_2$ mixture was photocatalytically active for the degradation of methyl orange in water, but its mass activity decreased with increasing the calcination temperature because of the formation of the photoinactive Zn_2TiO_4, Zn_2SnO_4 and $Zn_2Ti_{0.5}Sn_{0.5}O_4$. The sample became completely inert for the photocatalysis after prolonged calcination at 1300 °C (42 h) since all of the active component oxides were reacted to form the solid solution $Zn_2Ti_{0.5}Sn_{0.5}O_4$ with no photocatalytic activity. After the calcination at 500 °C for 2 h, the photocatalytic mass activity of the $ZnO/TiO_2/SnO_2$ mixture was 16.4 times that of SnO_2, 2.0 times that of TiO_2, and 0.92 times that of ZnO.

Acknowledgments

The authors would thank Profs. Ruji Wang, and Jianyuan Yu, Mr. Jingzhi Wei, and Yu Liang, Mrs. Xiaoyan Ye, Meijuan Zhao, and Feng'en Chen for their helps in the characterizations of the samples. We also thank the financial support of this work from NSF China (Grant: 20125310) and National Basic Research Program of China (Grant: 2003CB615804).

References

[1] M.R. Hoffmann, S.T. Martin, W.Y. Choi, D.W. Bahnemann, Chem. Rev. 95 (1995) 69–96.
[2] J. Yang, D. Li, X. Wang, X.J. Yang, L.D. Lu, J. Solid State Chem. 165 (2002) 193–198.
[3] L.Y. Shi, C.Z. Li, H.C. Gu, D.Y. Fang, Mater. Chem. Phys. 62 (2000) 62–67.
[4] G. Marcì, V. Augugliaro, M.J. López-Munoz, C. Martín, L. Palmisano, V. Rives, M. Schiavello, R.J.D. Tilley, A.M. Venezia, J. Phys. Chem. B 105 (2001) 1033–1040.
[5] J. Bandara, K. Tennakone, P.P.B. Jayatilaka, Chemosphere 49 (2002) 439–445.
[6] C. Wang, J.C. Zhao, X.M. Wang, B.X. Mai, G.Y. Sheng, P.A. Peng, J.M. Fu, Appl. Catal. B: Environ. 39 (2002) 269–279.
[7] Y.T. Kwon, K.Y. Song, W.I. Lee, G.J. Choi, Y.R. Do, J. Catal. 191 (2000) 192–199.
[8] K.Y. Song, M.K. Park, Y.T. Kwon, H.W. Lee, W.J. Chung, W.I. Lee, Chem. Mater. 13 (2001) 2349–2355.
[9] B. Pal, T. Hata, K. Goto, G. Nogami, J. Mol. Catal. A: Chem. 169 (2001) 147–155.
[10] F.H. Dulin, D.E. Rase, J. Am. Ceram. Soc. 43 (1960) 125–131.
[11] S.F. Bartram, R.A. Slepetys, J. Am. Ceram. Soc. 44 (1961) 493–499.
[12] J. Yang, J.H. Swisher, Mater. Charact. 37 (1996) 153–159.
[13] W. Chaisan, R. Yimnirun, S. Ananta, D.P. Cann, J. Solid State Chem. 178 (2005) 613–620.
[14] K. Zakrzewska, Thin Solid Films 391 (2001) 229–238.
[15] H.P. Naidu, A.V. Virkar, J. Am. Ceram. Soc. 81 (1998) 2176–2180.
[16] M.M. Oliveira, D.C. Schnitzler, A.J.G. Zarbin, Chem. Mater. 15 (2003) 1903–1909.
[17] F. Fresno, J.M. Coronado, D. Tudela, J. Soria, Appl. Catal. B: Environ. 55 (2005) 159–167.
[18] T. Hashemi, H.M. Al-allak, J. Illingsworth, A.W. Brinkman, J. Woods, J. Mater. Sci. Lett. 9 (1990) 776–778.
[19] W.B. White, B.A. Deangelis, Spectrochim. Acta 23A (1967) 985–995.
[20] G.T.K. Fey, D.L. Huang, Electrochim. Acta 45 (1999) 295–314.
[21] M. Ocana, W.P. Hsu, E. Matijević, Langmuir 7 (1991) 2911–2916.
[22] C. Wang, X.M. Wang, J.C. Zhao, B.X. Mai, G.Y. Sheng, P.A. Peng, J.M. Fu, J. Mater. Sci. 37 (2003) 2989–2996.
[23] F.Q. Huang, R.C. Somers, A.D. McFarland, R.P.V. Duyne, J.A. Ibers, J. Solid State Chem. 174 (2003) 334–341.
[24] A. Hagfeldt, M. Grätzel, Chem. Rev. 95 (1995) 49–68.
[25] W. Spence, J. Appl. Phys. 38 (1967) 3767–3770.
[26] D. Davazoglou, Thin Solid Films 302 (1997) 204–213.
[27] E.K. Shokr, M.M. Wakkad, H.A.A. El-Ghanny, H.M. Ali, J. Phys. Chem. Solids 61 (2001) 75–85.
[28] C. Wang, X.M. Wang, B.Q. Xu, J.C. Zhao, B.X. Mai, P.A. Peng, G.Y. Sheng, J.M. Fu, J. Photochem. Photobiol. A: Chem. 168 (2004) 47–52.
[29] A.L. Linsebigler, G.Q. Lu, J.T. Yates Jr., Chem. Rev. 95 (1995) 735–785.
[30] P.V. Kamat, Chem. Rev. 93 (1993) 267–300.